

Supplementary Information

Interface engineering of solution processed hybrid organohalide perovskite solar cells

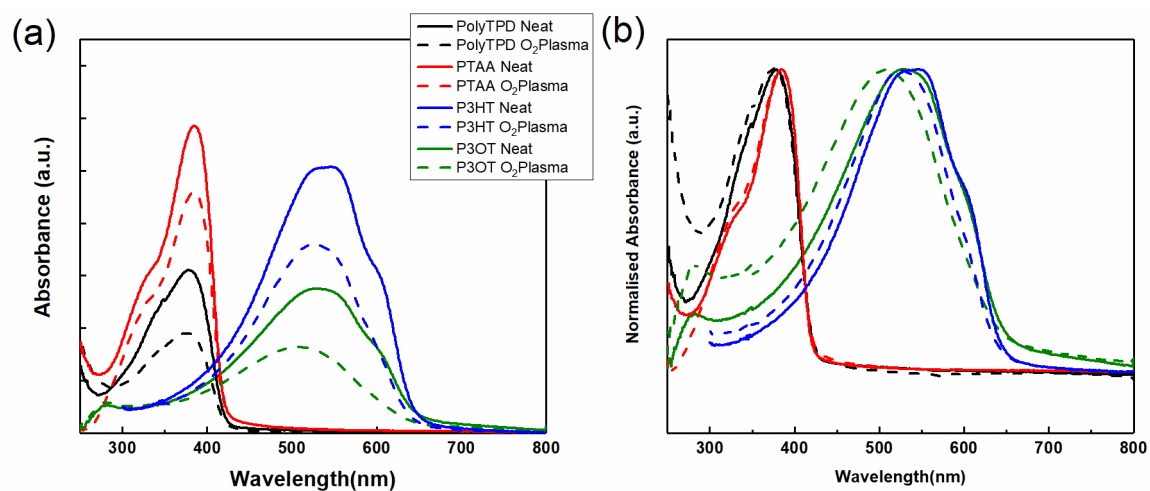
Shanshan Zhang^{1,2}, Martin Stolterfoht², Ardalan Armin³, Qianqian Lin⁴, Fengshuo Zu^{5,6}, Jan Sobus¹, Hui Jin¹, Norbert Koch^{5,6}, Paul Meredith³, Paul L Burn^{1,*}, Dieter Neher^{2,*}

1. Centre for Organic Photonics & Electronics (COPE), School of Chemistry and Molecular Biosciences, The University of Queensland, Brisbane 4072, Australia
2. Institute of Physics and Astronomy, University of Potsdam, Karl-Liebknecht-Str. 24-25, D-14476 Potsdam-Golm, Germany.
3. Department of Physics, Swansea University, Singleton Park, Swansea SA2 8PP Wales, United Kingdom
4. Key Lab of Artificial Micro-and Nano-Structures of Ministry of Education of China, School of Physics and Technology, Wuhan University, Wuhan, 430072, P. R. China
5. Institut für Physik & IRIS Adlershof, Humboldt-Universität zu Berlin, 12489 Berlin, Germany
6. Helmholtz-Zentrum Berlin für Materialien und Energie GmbH, 12489 Berlin, Germany

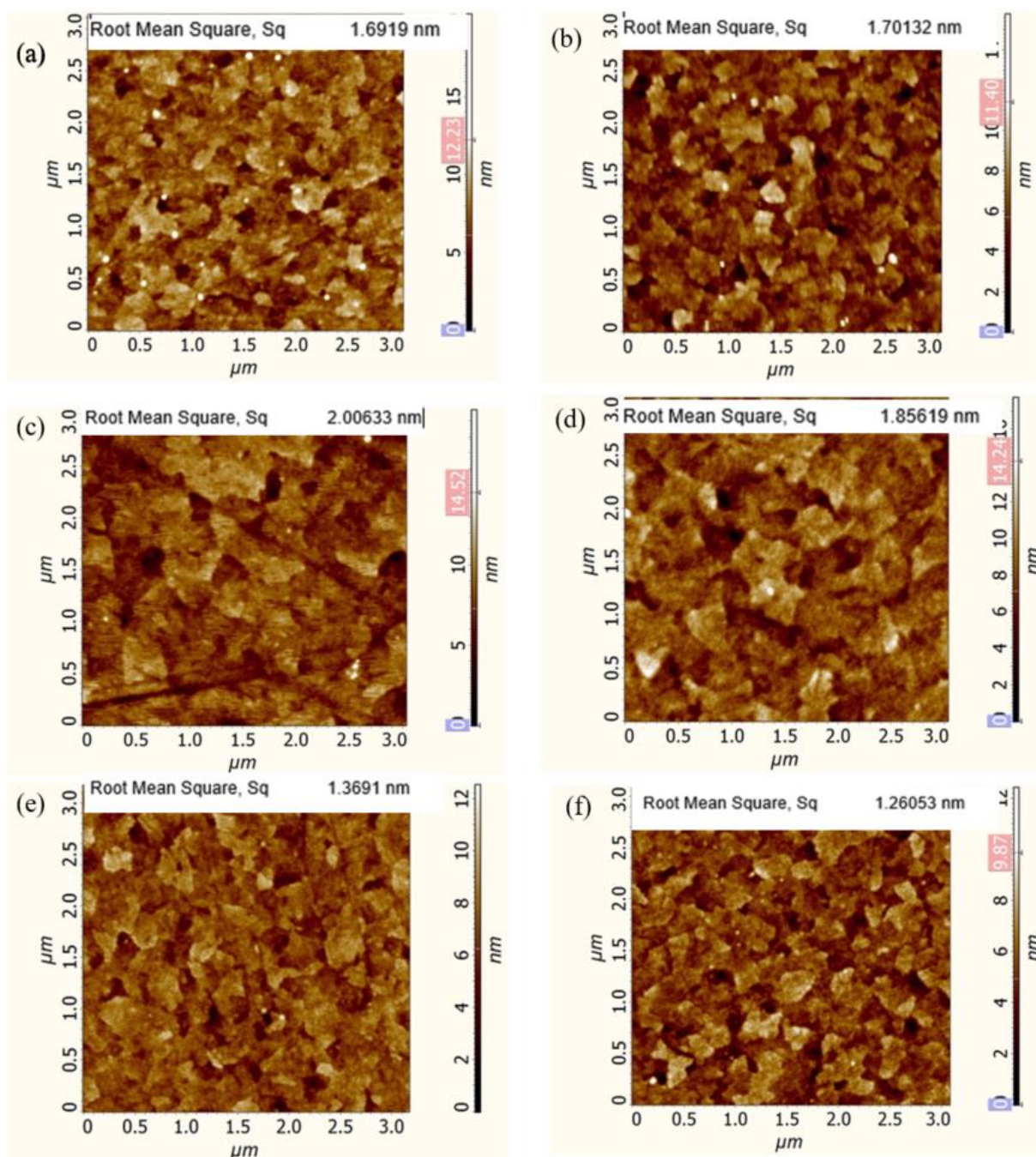
*Requests for materials and all correspondence should be addressed to:

neher@uni-potsdam.de; p.burn2@uq.edu.au

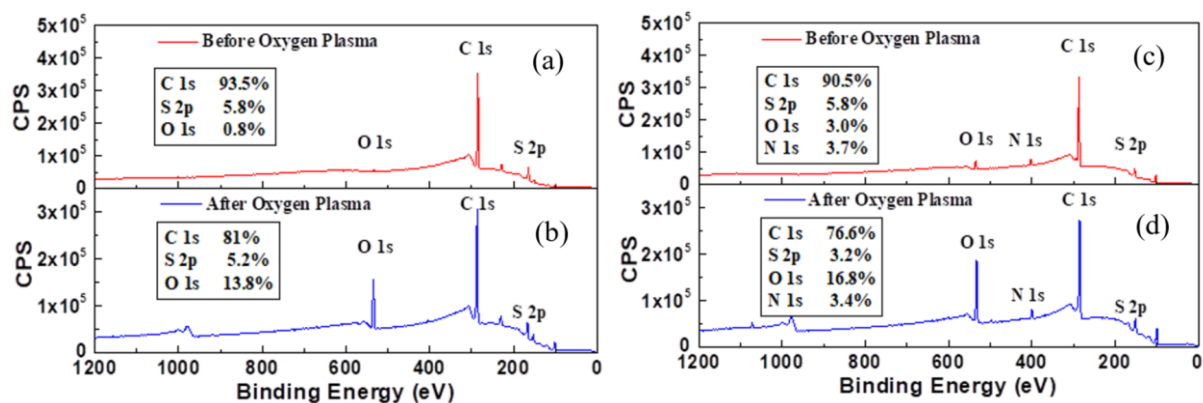
1. Supporting figures:



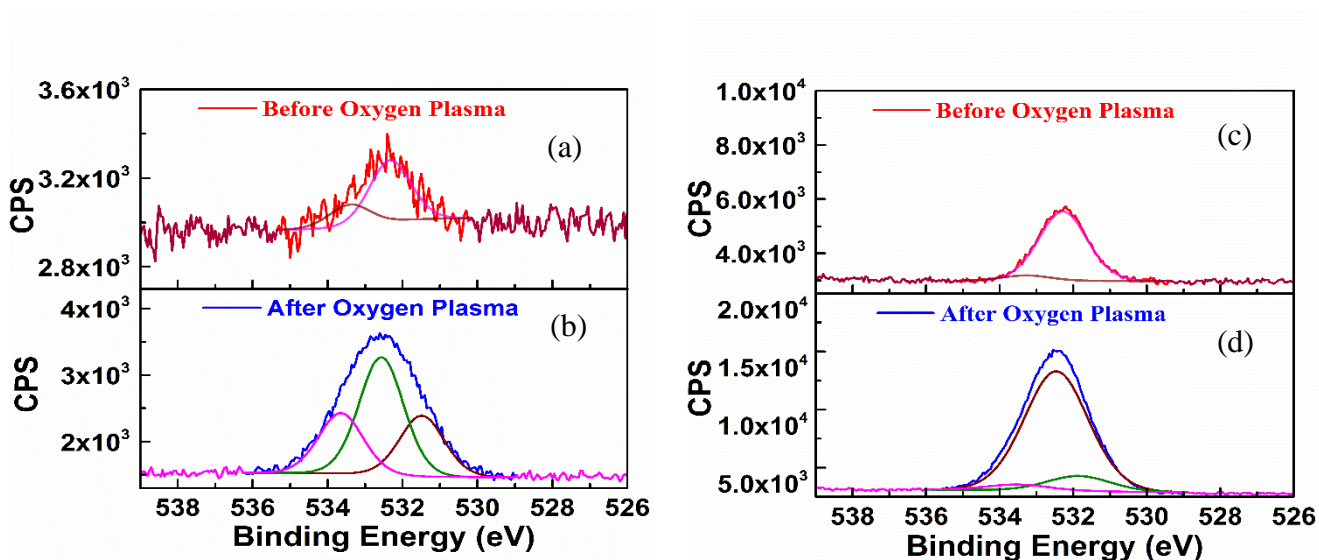
Supplementary Figure S1. Original and peak normalized UV-vis spectra of different polymers used as interlayers original (a) and normalized (b) at before and after the oxygen plasma treatment of 5 seconds.



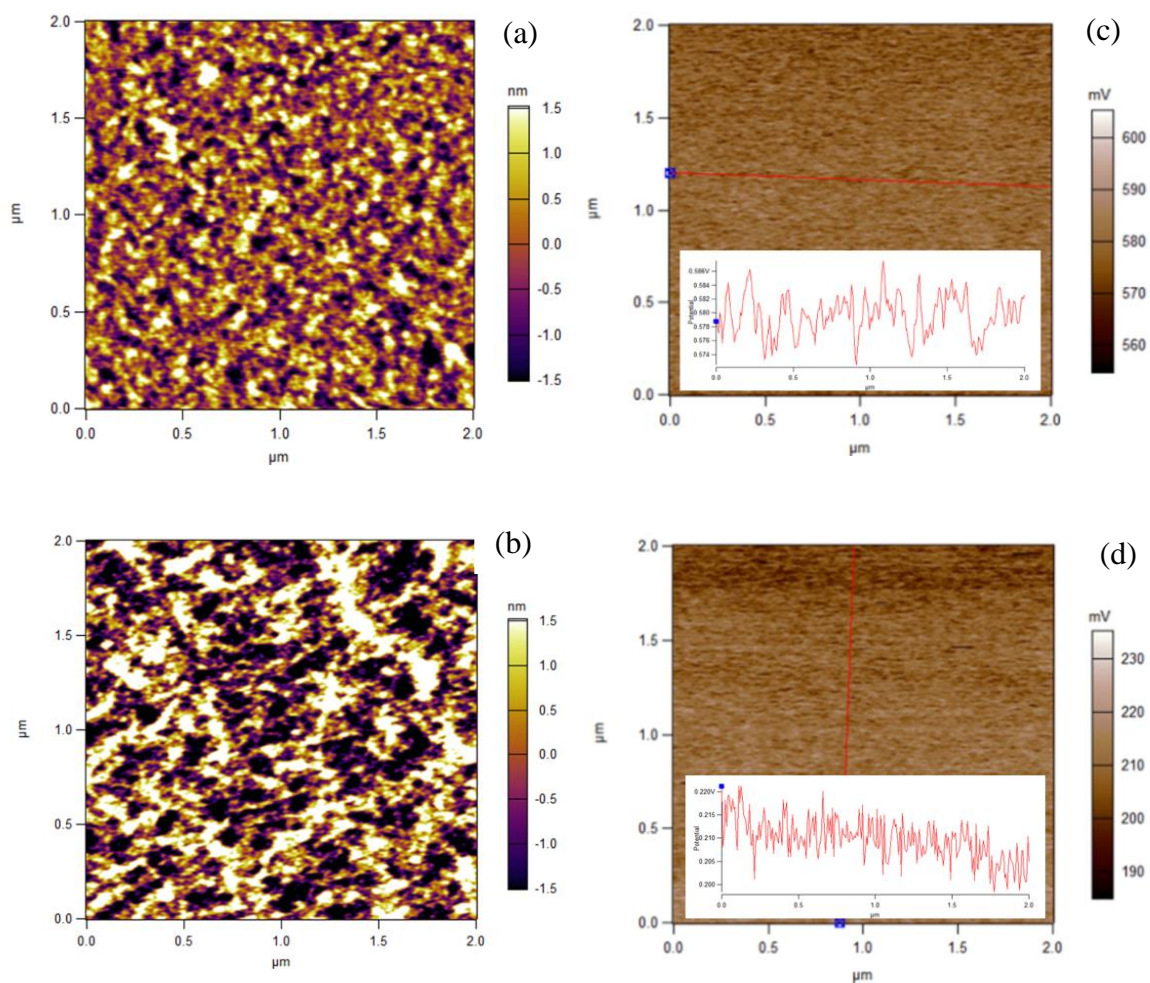
Supplementary Figure S2. Atomic Force Microscopy (AFM) images ($3 \times 3 \mu\text{m}$) of PolyTPD, P3OT and PTAA films before and after plasma treatment. Topography of a PolyTPD neat film before (a) and after plasma treatment (b); P3OT neat film before (c) and after plasma treatment (d); PTAA neat film before (e) and after plasma treatment (f). The bars next to the individual panels represent the height profile of the scanned area. The similar root mean square surface roughness demonstrates that the oxygen plasma treatment did not alter the roughness within the measurement error.



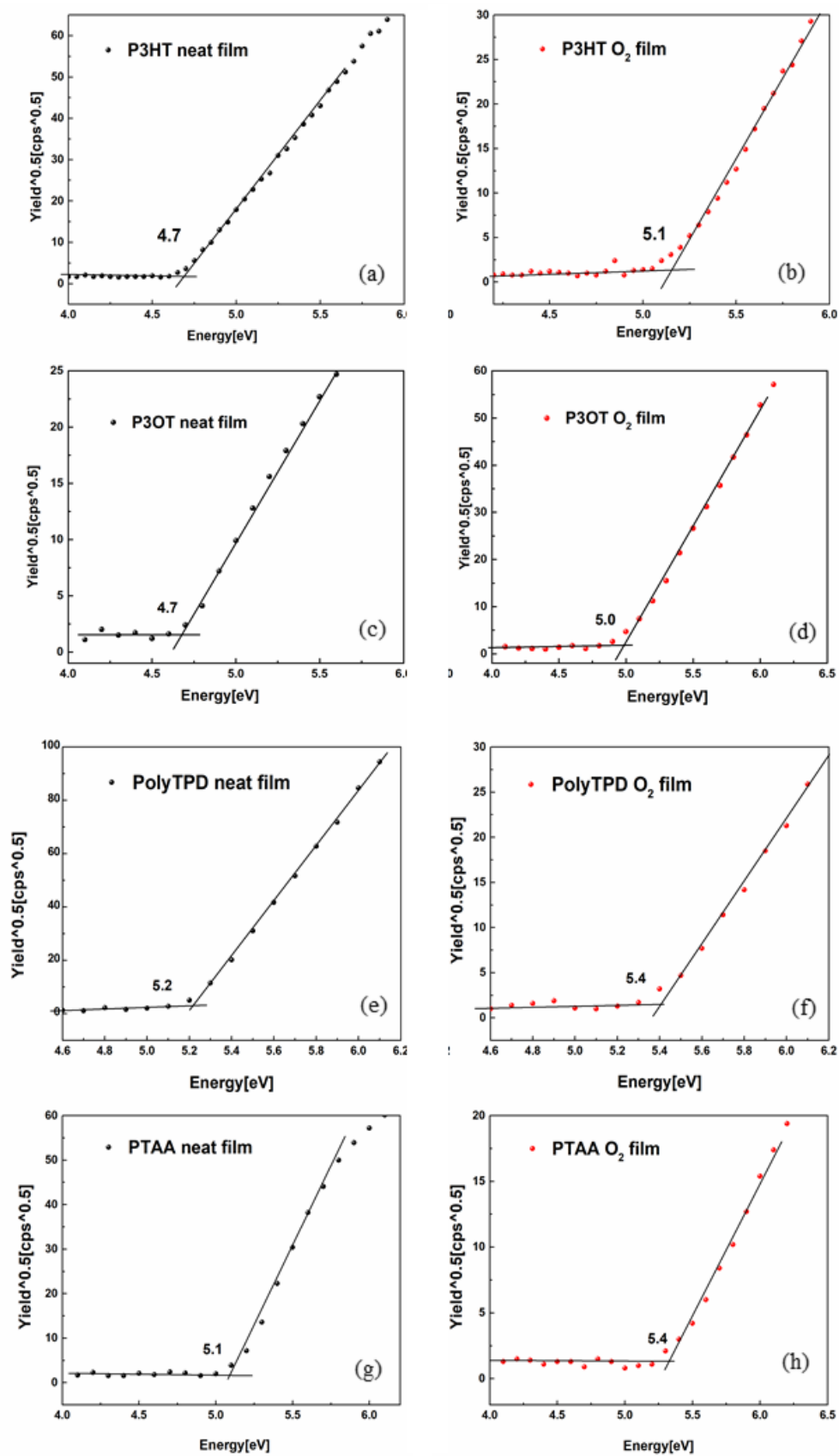
Supplementary Figure S3. X-ray Photoelectron Spectroscopy (XPS) spectra of a P3OT films (a) before and (b) after 5 seconds oxygen plasma treatment; A PolyTPD films (c) before and (d) after 5 seconds oxygen plasma treatment



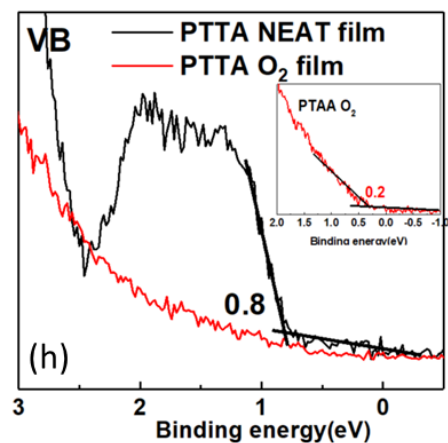
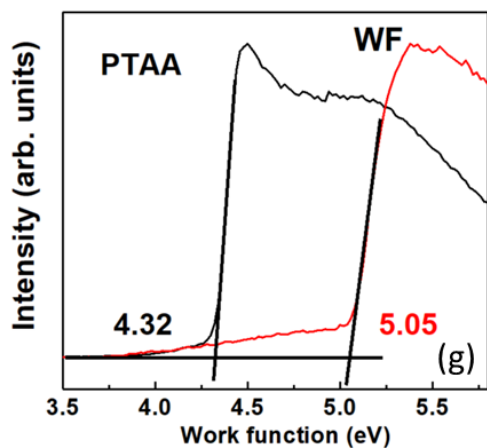
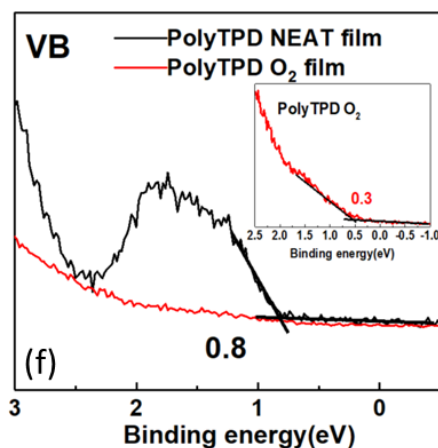
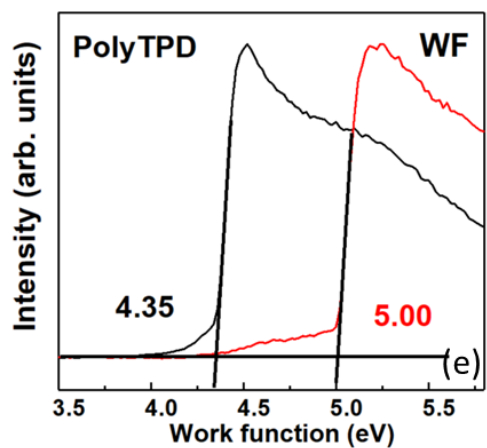
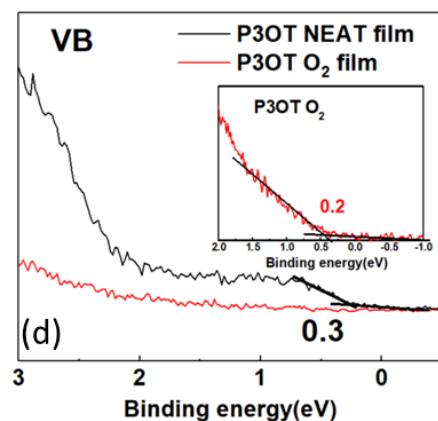
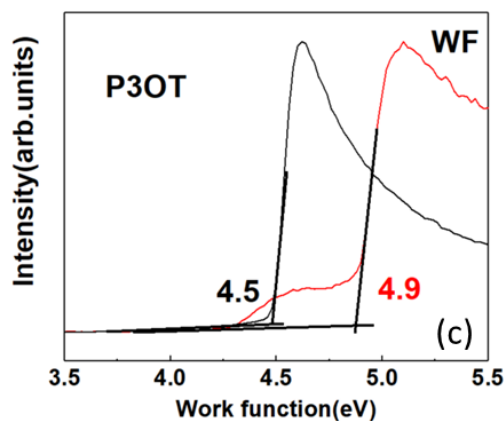
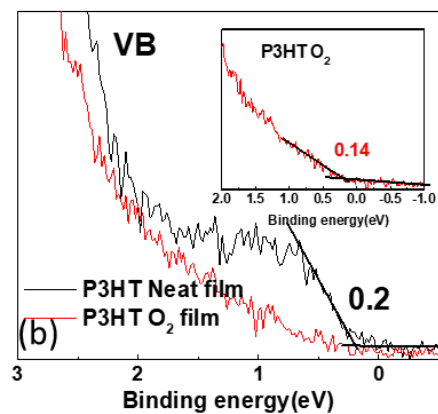
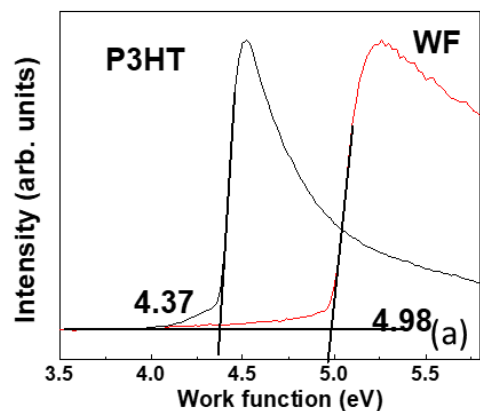
Supplementary Figure S4. (a, b) XPS spectra of the O1s region for a neat and O₂ plasma treated P3HT film, respectively; similarly, (c, d) show the XPS spectra of the O1s region for a neat and O₂ plasma treated PTAA film, respectively. Also shown are Gaussian fits at different bindings energies which indicate O-C=O, O=C, O-C, and /or O-S bonds for the P3HT film, and O=C bonds for the PTAA film.



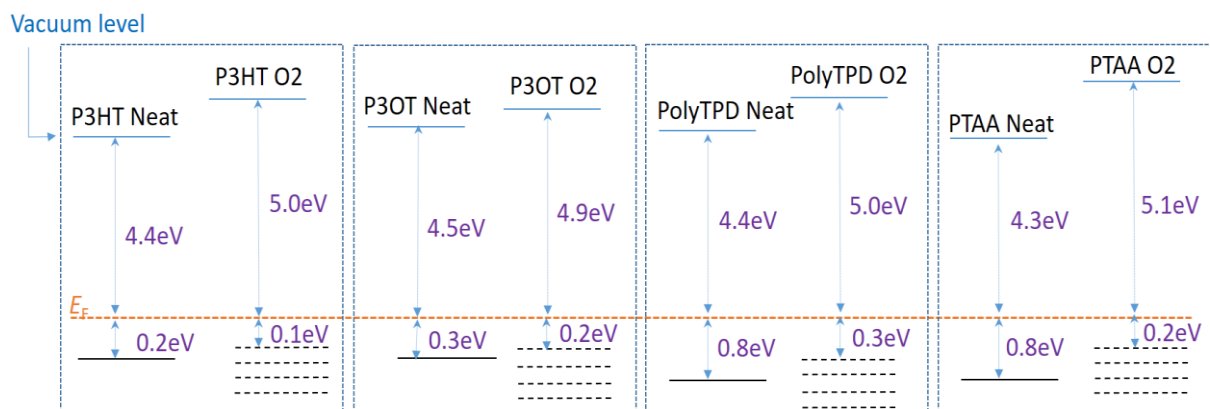
Supplementary Figure S5. AFM and Scanning Kelvin Probe Microscopy (SKPM) images ($2 \times 2 \mu\text{m}$) of P3HT films. Topography of a P3HT neat film before (a) and after plasma treatment (b). SKPM image of a P3HT neat film before (c) and after plasma treatment (d). The insets in (c) and (d) show the potential along the red line of the corresponding films.



Supplementary Figure S6. Photoelectron yield spectroscopy spectra of a (a) P3HT neat film and treated film (b); (c) P3OT neat film and treated film (d); (e) Poly TPD neat film and treated film (f); (g) PTAA neat film and treated film (h).



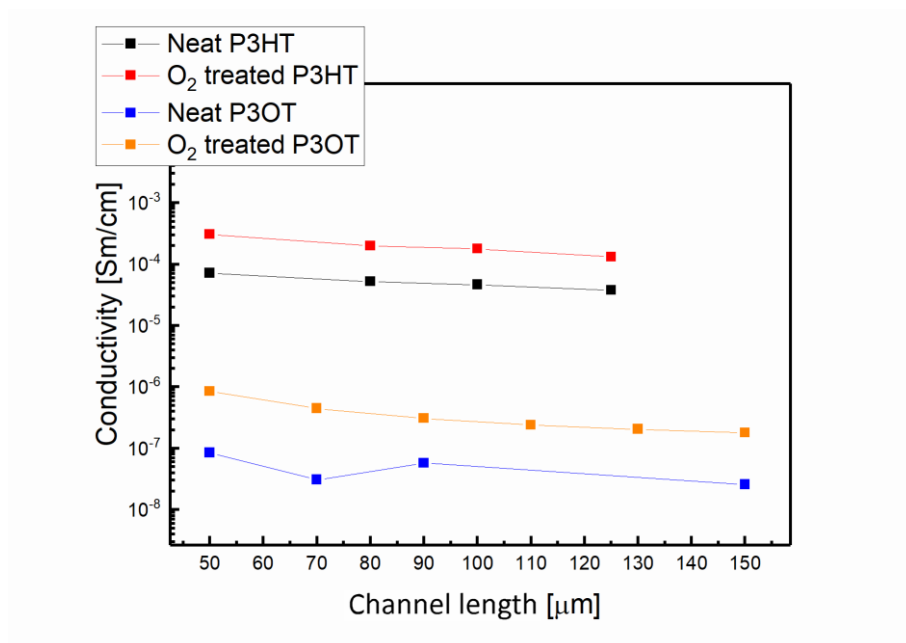
Supplementary Figure S7. Work function changes measured by using ultraviolet photoelectron spectroscopy (UPS) of (a) P3HT; (c) P3OT; (e) PolyTPD and (g) PTAA films before the oxygen plasma treatment; The O₂-treatment induced changes of the highest occupied molecular orbitals of (b) P3HT; (d) P3OT; (f) PolyTPD and (h) PTAA films after the oxygen plasma treatment. We note that only an upper IP limit can be specified for the treated films due to the uncertainty in the determination of the valance band onset.



Supplementary Figure S8. Energy levels derived from the UPS measurements of the four polymers before and after the oxygen plasma treatment by assuming a fixed Fermi-level during the measurement. We note that only an upper IP limit can be specified for the treated films due to the uncertainty in the determination of the valance band onset.

	UPS (Work function)				UPS (Ionization Potential)			
	P3HT	P3OT	Poly TPD	PTAA	P3HT	P3OT	Poly TPD	PTAA
Neat film	4.4eV	4.5eV	4.4eV	4.3eV	4.6eV	4.8eV	5.2eV	5.1eV
Treated film	5.0eV	4.9eV	5.0eV	5.1eV	5.1eV	5.1eV	5.3eV	5.3eV

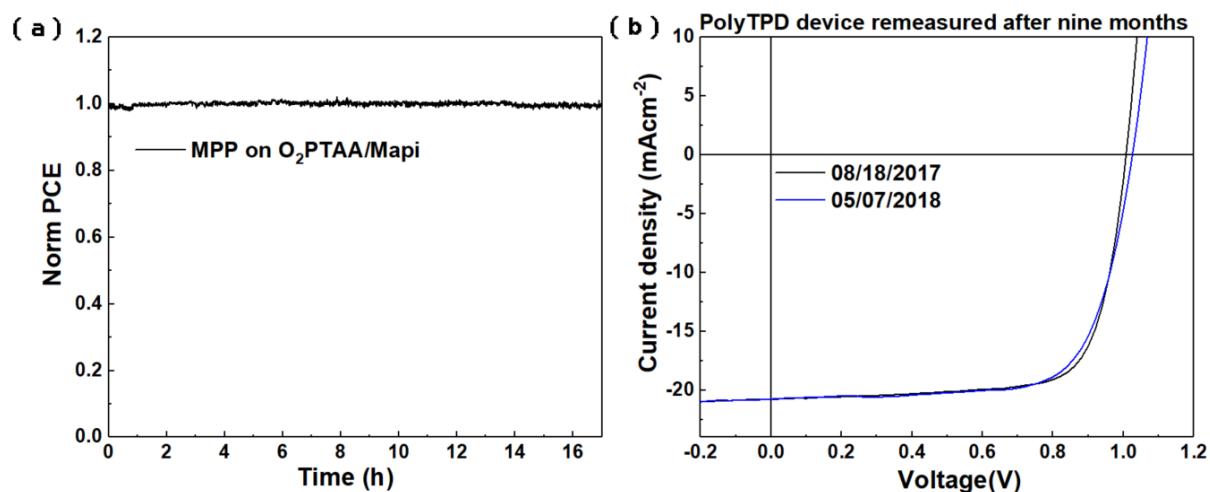
Table S1. Change in work function and ionization potential (IP) of different polymer layers measured using Ultraviolet photoelectron spectroscopy (UPS) before and after oxygen plasma treatment. We note that only an upper IP limit can be specified due to the uncertainty in the determination of the valance band onset as shown in Supplementary Figure S7.



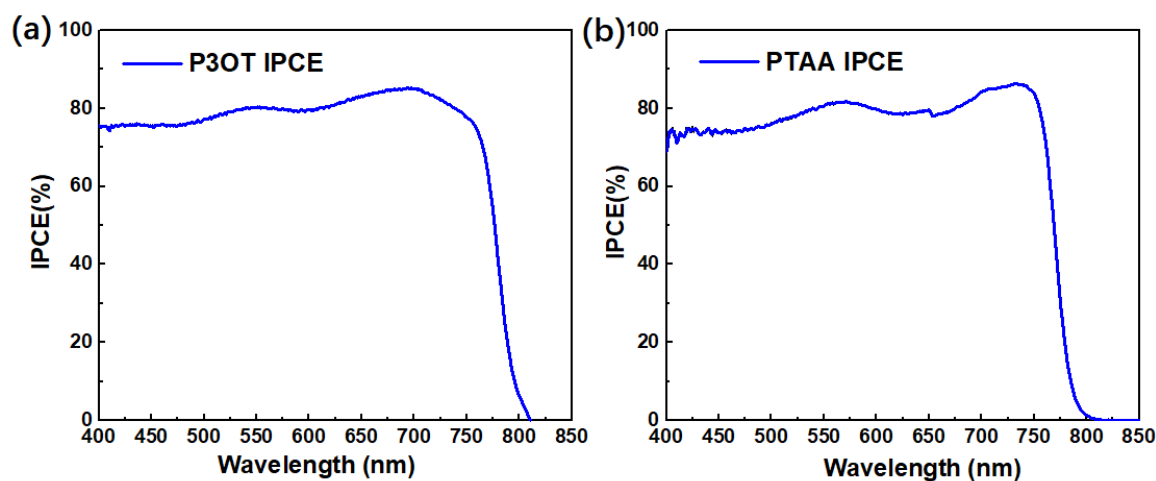
Supplementary Figure S9. *The electrical conductivity of poly(thiophene) HTLs as a function of channel width showing an increase upon the oxygen plasma treatment by 1 order of magnitude.*



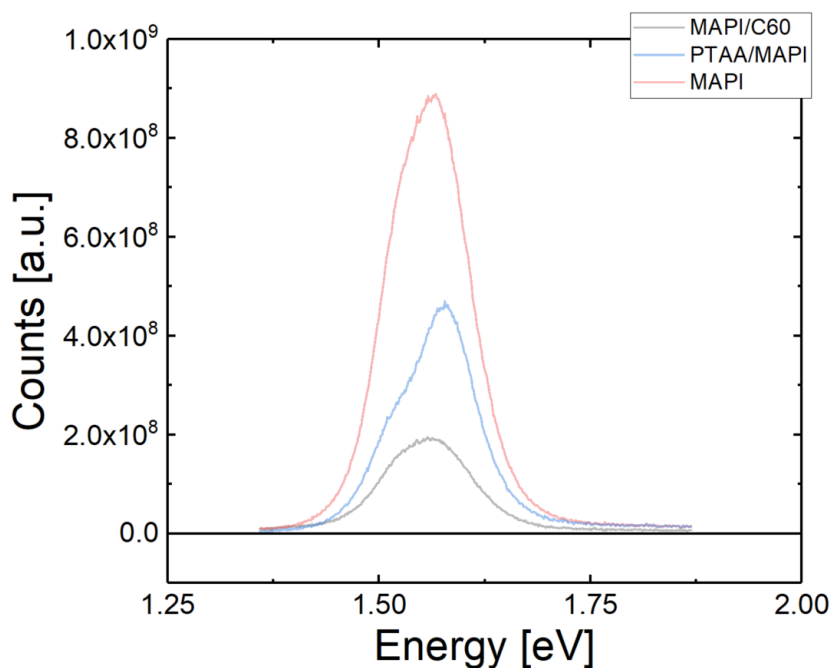
Supplementary Figure S10. *Perovskite films deposited on PTAA with and without plasma treatment.*



Supplementary Figure S11. *Stability measurements on devices; (a) maximum power point tracking on a perovskite cell with oxygen treated PTAA as hole transporting layer; (b) JV characteristics of a PolyTPD device before and after nine months.*



Supplementary Figure S12. *Incident Photon to Electron Conversion Efficiency (IPCE) spectra of the plasma treated P3OT (a) and PTAA (b) interlayer $\text{CH}_3\text{NH}_3\text{PbI}_3$ perovskite devices.*



Supplementary Figure S13. Photoluminescence spectra of neat MAPI, MAPI/C60, and plasma treated PTAA/MAPI films on glass. The films were excited with a 445 nm continuous wave laser with a 1 sun equivalent intensity that produces a short-circuit current density of $\sim 22 \text{ mA cm}^{-2}$. The addition of a charge transport layer clearly quenches the photoluminescence due to additional non-radiative interface recombination losses. However, the graph indicates less losses at the treated PTAA/perovskite interface compared to the MAPI/C60 interface, which further suggests that the O_2 -plasma treatment itself is not causing additional interfacial recombination.